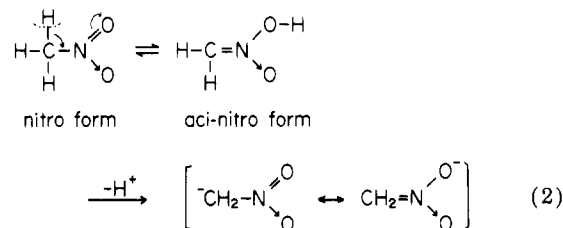


Figure 10. Infrared spectra of adsorbed CH_3NO_2 on dehydroxylated (a, b) and hydroxylated (c, d) ZnO surfaces. Broken and solid lines have the same meanings as in Figure 7.

versible adsorption of such a molecule might occur owing to a stronger interaction with induced dipoles of the molecules, in addition to the dispersion force. From the standpoint of the adsorption through the dispersion force, it may be reasonable to consider that horizontally oriented molecules are more stable than perpendicularly oriented ones on the solid surface. Actually, the molecular area occupied by adsorbed $n\text{-C}_7\text{H}_{16}$ is calculated to be 0.625 nm^2 based on the adsorption data (Figure 6), being very large compared with the value expected for the vertical orientation.

(d) CH_3NO_2 . The IR spectra of CH_3NO_2 adsorbed on the ZnO surface are illustrated in Figure 10. On the dehydroxylated surface, a broad and intense band centered at 3365 cm^{-1} appears, in addition to the CH stretching bands in the range $2972\text{--}2852 \text{ cm}^{-1}$. The band at 3365 cm^{-1} should be assigned to the OH stretching vibrations, since the OD band was clearly observed around 2500 cm^{-1} when deuterated nitromethane (CD_3NO_2) was adsorbed on the same sample. These facts substantiate the formation of

surface hydroxyl groups on the adsorption of CH_3NO_2 . It may be due to the electron-attractive nature of the nitro group, where the hydrogen atom attached to the carbon atom (α position) adjacent to the nitro group is easily activated to leave as a proton. CH_3NO_2 is a compound exhibiting tautomerism (eq 2), in which the *aci*-nitro form



($\text{p}K_a = 3.2$) is predominant in the presence of a proton acceptor.²⁸ On the dehydroxylated ZnO surface, the oxygen atom will attract this proton to produce hydroxyl groups, the remainder being linked to the surface zinc atom. The presence of $\text{C}=\text{N}$ bonding is confirmed by the band at 1630 cm^{-1} .²⁵ The formation of strong hydrogen bonding between adsorbed species will cause a perturbation of hydroxyl groups, resulting in a shift of the OH band toward lower frequencies.

On the hydroxylated surface, the bands for the CH_3 (2972 cm^{-1}) and NO_2 groups (1555 and 1370 cm^{-1}) are reduced by evacuation of the vapor, while the bands due to the CH_2 (2920 cm^{-1}) and $\text{C}=\text{N}$ groups (1630 cm^{-1}) remain distinct (Figure 10d). Furthermore, the free hydroxyl bands at 3695 and 3675 cm^{-1} disappeared through the adsorption of CH_3NO_2 . From these observations, it is reasonable to infer that CH_3NO_2 molecules can be adsorbed in the *aci*-nitro form on the free hydroxyl groups.

Acknowledgment. The present work was partly supported by a Grant-in-Aid for Scientific Research, No. 00547008, from the Ministry of Education, Science and Culture of Japanese Government.

(27) Manuscript to be submitted for publication.

(28) Imoto, M. "Yuki-Denshiron-Kaisetsu"; Tokyo Kagaku-Dojin: Tokyo, 1967.

Surface Tension of Lithium Fluoride and Beryllium Fluoride Binary Melt

Kunimitsu Yajima,* Hirotake Moriyama, Jun Oishi, and Yasunobu Tomimaga

Department of Nuclear Engineering, Kyoto University, Kyoto 606, Japan (Received: December 14, 1981; In Final Form: June 28, 1982)

The surface tension of molten salt containing lithium fluoride and beryllium fluoride has been measured by the maximum bubble pressure method. The surface tension isotherm has a minimum at about 40 mol % of beryllium fluoride, which might be due to the formation of complex ions. An empirical equation of the surface tension of molten halides is introduced, and the surface tension of lithium fluoride-beryllium fluoride binary melt is explained with this equation, taking the formation of tetrafluoroberyllate complex ion in a surface layer into consideration.

Introduction

Molten salts are useful materials from the viewpoint of their physical and chemical merits. In particular, $\text{LiF}\text{--}\text{BeF}_2$ binary melt is expected to be applied to numerous fields in nuclear engineering, for example, to the fuel-solvent of molten salt breeder reactors. The properties of $\text{LiF}\text{--}\text{BeF}_2$ binary melt have been measured vigorously for

many years,^{1,2} but the interfacial properties such as the surface tension are known little in spite of their importance.³ The surface phenomena are also of interest with

(1) K. A. Romberger, J. Braunstein, and R. E. Thoma, *J. Phys. Chem.*, **76**, 1154 (1972).

(2) F. Vaslow and A. H. Narten, *J. Chem. Phys.*, **59**, 4949 (1973).

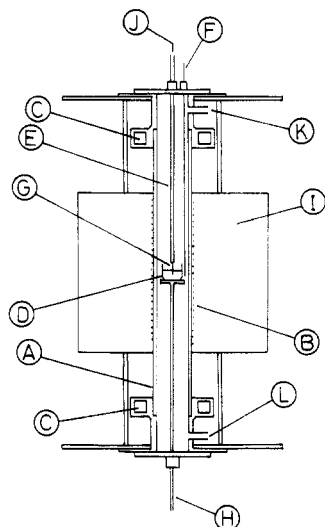


Figure 1. Experimental apparatus: (A) furnace tube; (B) Kanthal resistance heater; (C) water-cooling jacket; (D) crucible; (E) bubble tube; (F) thermocouple; (G) capillary tube; (H) crucible support; (I) insulator; (J) argon gas inlet; (K) argon gas outlet; (L) to vacuum.

respect to the microscopic structure of the liquid.

The purpose of this study is to investigate the temperature and composition dependences of the surface tension of LiF-BeF₂ binary melt and to discuss its microscopic behavior.

Experimental Section

The maximum bubble pressure method⁴ was applied for determining the surface tension, because of the simplicity and the precision of the measurement at high temperatures in a moderately corrosive liquid.

Apparatus. The electric furnace to melt salts is shown in Figure 1. A furnace tube of alumina (100-mm inner diameter, 5 mm thick and 1000 mm long) was wound with a Kanthal resistance heater. Top and bottom lids of stainless steel with a water-cooling jacket were installed at the furnace tube. A 100-cm³ nickel crucible containing a sample melt was set in the central part of the furnace tube. A bubble tube of stainless steel and a chromel-alumel thermocouple covered with an Inconel sheath were attached to the top lid with a O-ring seal. A capillary tube of nickel (2-mm outer diameter, 0.2 mm thick and 40 mm long) sharpened to a knife edge at the tip was welded at the lower end of the bubble tube.

The temperature of the system was controlled within 0.025 °C with a voltage stabilizer manufactured by Eikoh Electric, Ltd. The working gas was a purified argon which, prior to use, was passed through chemical traps filled with molecular sieve and titanium sponges to remove possible H₂O, N₂, and O₂ contaminations. The pressure of the working gas bubble was measured with a manometer filled with dibutyl phthalate.

Procedures. LiF and BeF₂ of pure grade, obtained from Nakarai Chemicals Ltd., were subjected to preliminary dehydration. Known amounts of LiF and BeF₂ were put into the crucible and dried by evacuating at 200 °C for 1 day in the furnace.

The furnace was filled with the working gas, and the temperature was raised above the melting point of the sample melt and kept constant by a temperature-controlling device.

TABLE I: Density of LiF-BeF₂ Binary Melt^{6,7}

composition, mol %			$\rho(\text{g cm}^{-3}) = a - bt(^{\circ}\text{C})$	
LiF	BeF ₂	temp range, °C	a	10 ⁴ b
100	0	850-1000	2.199	4.533
90	10	800-900	2.131	4.100
80	20	725-825	2.156	4.200
69	31	500-800	2.168	4.133
66.67	33.33	450-900	2.166	3.800
56.67	43.33	450-900	2.243	4.475
50	50	525-900	2.241	4.500
45	55	450-800	2.130	3.629 ^a
25.1	74.9	581.2-861.5	2.093	2.39
10.8	89.2	743.5-858.0	2.035	1.48
0.0	100.0	850		1.96 ^b

^a ± 1%; ref 6. ^b ± 0.4%; ref 7.

TABLE II: Surface Tension of LiF-BeF₂ Binary Melt

composition, mol %			$\gamma(\text{dyn cm}^{-1}) = a - bt(^{\circ}\text{C})$	
LiF	BeF ₂	temp range, °C	a	b
100	0	910-970	343.4 ^a	0.109 ^a
85	15	784-943	308	0.12
75	25	725-842	293	0.13
67	33	500-800	263	0.12
50	50	558-794	265	0.12
33	67	702-786	288	0.13
67	33		260 ^b	0.12 ^b

^a Taken from ref 18. See text. ^b Taken from ref 3. Errors are +30% and -10%.

Then the bubble tube was lowered gradually, while the working gas was blown from the capillary tip. When the tip came in touch with the free surface of the melt, a sudden increase of the pressure of the gas in the bubble tube was observed. By this observation the free surface of the melt was located. After a further immersion of the capillary, the maximum gas pressure necessary to liberate a gas bubble formed at the tip was measured within 0.5 mm of the manometer liquid reading. The measurements were made with varying immersion depth of the capillary tip.

The radius of the capillary tip was calibrated within 0.001 mm by preliminary measurements of the surface tension of water.

Results

According to Schrödinger⁴ the surface tension γ of the sample melt is calculated from

$$\gamma = \frac{1}{2}r\rho gh[1 - \frac{2}{3}(r/h) - \frac{1}{6}(r/h)^2] \quad (1)$$

where r is the radius of the capillary tip, h is $(\rho_m l_m - \rho l)/\rho$, ρ and ρ_m are the densities of the sample melt and the manometer liquid, respectively, l is the immersion depth of the capillary tip, l_m is the measured manometer reading, and g is the acceleration due to gravity.

The density ρ_m in g cm⁻³ of dibutyl phthalate used as a manometer liquid satisfies⁵

$$\rho_m = 1.0619 - 0.000801t \quad (2)$$

where t is the temperature in °C. The experimental error of ρ_m was reported to be ±0.0005 g cm⁻³. The typical density equations of LiF-BeF₂ binary melt are arranged in Table I.^{6,7} The density at any composition was inter-

(3) S. Cantor, J. M. Cooke, A. S. Dworkin, G. D. Robins, R. S. Thoma, and G. M. Watson, U.S. Atomic Energy Commission Report ORNL-TM-2316, Aug 1968.

(4) E. Schrödinger, *Ann. Phys. (Leipzig)* **46**, 413 (1915).

(5) A. I. Kemppinen and N. A. Gokcen, *J. Phys. Chem.*, **60**, 126 (1956).

(6) B. C. Blanke, E. N. Bousquet, M. L. Curtis, and E. L. Murphy, U.S. Atomic Energy Commission Report MLM-1086, March 1959.

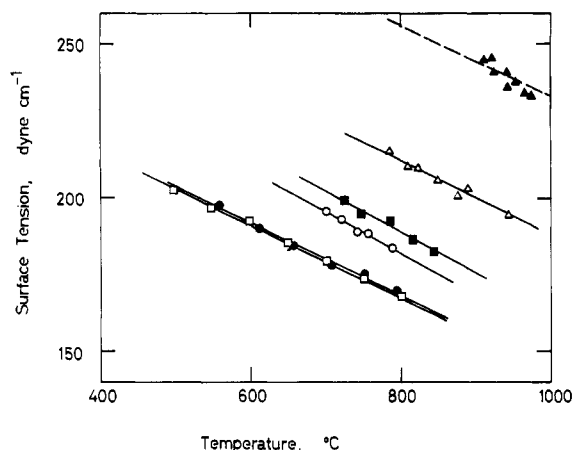


Figure 2. Temperature dependence of surface tension of LiF-BeF₂ binary melt. Mol % of BeF₂ is (▲) 0%, (△) 15%, (■) 25%, (□) 33%, (●) 50%, and (○) 67%. The solid and broken lines are drawn from empirical equations of this work and ref 18, respectively.

polated by assuming that the molar volume of the mixture is linearly dependent on the composition. The thermal expansion of the capillary tip was taken into account.

The measured values of surface tension are shown in Figure 2. The empirical equations were obtained by the method of least squares assuming linear temperature dependence and are summarized in Table II. The empirical equation for the pure LiF melt was taken from the literature¹⁵ because the temperature range used in this work was too narrow. The experimental error was estimated to be $\pm 3\%$ at most. A satisfactory agreement can be seen between the present study and previous work as to 67% LiF-33% BeF₂ melt.³

Discussion

Figure 3 shows that the surface tension isotherm of the LiF-BeF₂ binary melt at 800 °C exhibits a large negative deviation from additive behavior and has a minimum at about 40 mol % of BeF₂. Recently Desyatnik et al.⁹ found a similar feature of the surface tension isotherm for NaF-BeF₂ binary melt and they attributed the pronounced deviation to the formation of complex ions because of the strong polarizing power of Be²⁺.

Several theoretical treatments^{10,11} have been proposed to elucidate a negative deviation of the surface tension of the melt mixtures. However, their objects were mainly to evolve a model which would allow the prediction of the surface tension of the melt mixture based on the known surface tension of each component. On the other hand, some quantitative predictions of surface tension based on the Fowler-Kirkwood-Buff model have been made for not only Lennard-Jones fluids but also molten salts. In spite of an abrupt change in surface density profile, this model is shown to give a fairly reasonable interpretation of ex-

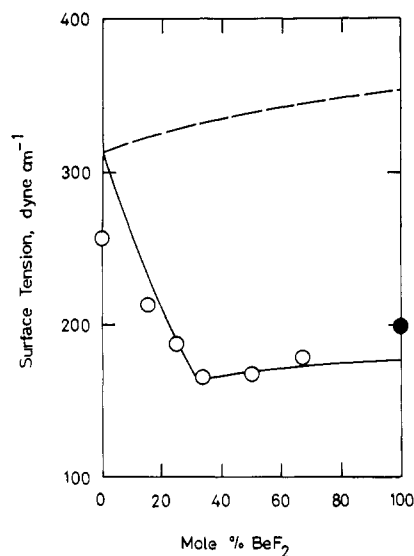


Figure 3. Composition dependence of surface tension of LiF-BeF₂ binary melt at 800 °C. Open circles show the values in this work and the closed circle gives the estimated value of ref 8. The broken and solid curves show theoretical values. See text.

perimental results for Lennard-Jones fluids.¹² As for molten salts, Goodisman et al.¹³⁻¹⁵ have claimed that this model should be applied together with the modified bulk radial distribution function. Unfortunately, our knowledge of the radial distribution function is not sufficient to apply the treatment of Goodisman et al. to the present system. In order to compare the results for the present system with those for the other systems, we will introduce here a new empirical equation.

According to the statistical investigation by Kirkwood and Buff¹⁶ following that by Fowler¹⁷ the surface tension γ of a liquid is given by

$$\gamma = \frac{\pi}{8} n^2 \int_0^\infty r^4 \frac{d\phi(r)}{dr} g(r) dr \quad (3)$$

where n is the number density of constituent particles composing the liquid, r is the distance between two particles, $\phi(r)$ is the interparticle pair potential, and $g(r)$ is the radial distribution function.

The surface tension of molten salt results mainly from the Coulomb force and the short-range repulsive force. The Coulomb component γ_c of the surface tension for a multicomponent system is expressed as follows by substituting $z_i z_j e^2 / r$ for $\phi(r)$ in eq 3:

$$\gamma_c = \frac{\pi}{8} \sum_{i,j} n_i n_j \int_0^\infty r^4 (-z_i z_j e^2 / r^2) g_{ij} dr \quad (4)$$

where n_i and n_j are the number densities of the ions having the electric charges z_i and z_j , respectively, and g_{ij} is the radial distribution function corresponding to ion pairs, i and j .

Together with the condition of electric neutrality, that is, $\sum_i z_i n_i = 0$, eq 4 is reduced to a simple form¹³

$$\gamma_c = -(e^2 / 32) \sum_i z_i (-z_i) n_i \quad (5)$$

Equation 5 shows that γ_c is obtained only by summing up the Coulomb forces between an arbitrary central ion having the charge of z_i and the surrounding charge which is defined as total charge around the central ion and is reduced statistically to $-z_i$ under the condition of electric neutrality.

Another important component of the surface tension γ_s due to the short-range repulsive force is considered to reduce the Coulomb component to the actual value of surface tension. For simplicity, eq 5 is modified with an

(7) S. Cantor, W. T. Ward, and C. T. Moynihan, *J. Chem. Phys.*, **50**, 2874 (1969).

(8) J. D. Mackenzie, *J. Chem. Phys.*, **32**, 1150 (1960).

(9) V. N. Desyatnik, N. M. Emelyanov, and E. I. Tomlin, *Russ. J. Phys. Chem. (Engl. Transl.)*, **59**, 422 (1979).

(10) G. Bertozzi and G. Sternheim, *J. Chem. Phys.*, **70**, 1838 (1966).

(11) D. A. Nissen and R. W. Carlsten, *J. Electrochem. Soc.*, **121**, 500 (1974).

(12) P. D. Shoemaker, G. W. Paul, and L. E. M. De Chazal, *J. Chem. Phys.*, **52**, 491 (1970).

(13) R. W. Pastor and J. Goodisman, *J. Chem. Phys.*, **68**, 3654 (1978).

(14) J. Goodisman, *J. Chem. Phys.*, **69**, 5341 (1978).

(15) J. Goodisman, *J. Chem. Phys.*, **73**, 5844 (1980).

(16) J. G. Kirkwood and F. P. Buff, *J. Chem. Phys.*, **17**, 338 (1949).

(17) R. H. Fowler, *Proc. R. Soc. London, Ser. A*, **159**, 229 (1937).

(18) G. J. Janz, "Molten Salts Handbook"; Academic Press, New York, 1967.

TABLE III: ω Values of Typical Alkali and Alkaline-Earth Halides^a

halides	ω	
	at T_m^b	at $1.5T_m^b$
LiF	0.411	0.366
NaF	0.461	0.406
KF	0.495	0.430
LiCl	0.445	0.397
NaCl	0.502	0.350
KCl	0.556	0.427
RbCl	0.609	0.444
CaCl ₂	0.468	0.430
SrCl ₂	0.567	0.525
CaBr ₂	0.442	0.388
SrBr ₂	0.579	0.553

^a From the surface tensions in ref 18. ^b T_m represents the melting temperature in K.

TABLE IV: ω Values of Binary Halide Systems at 1123 K^a

halides	ω	halides	ω
NaCl-SrCl ₂	0.506-0.566	RbCl-BaCl ₂	0.510-0.631
KCl-SrCl ₂	0.490-0.566	CsCl-BaCl ₂	0.501-0.631
RbCl-SrCl ₂	0.484-0.569	NaBr-BaBr ₂	0.509-0.651
CsCl-SrCl ₂	0.454-0.576	KBr-BaBr ₂	0.547-0.651
NaCl-BaCl ₂	0.506-0.631	RbBr-BaBr ₂	0.525-0.651
KCl-BaCl ₂	0.520-0.631	CsBr-BaBr ₂	0.513-0.651

^a From the surface tensions in ref 10.

empirical parameter showing the extent to which γ_c is compensated. In this case, the surrounding charge $-z_i$ in eq 5 is considered to be in either of the following two states. One is the state in which the surrounding charge is in contact with the central ion. The surrounding charge in this state exerts not only the Coulomb force but also the short-range repulsive force with the central ion and the two forces are fairly compensated. Thus, this surrounding charge may be almost ineffective with regard to the surface tension. The other is the state in which the surrounding charge is separated from the central ion and this surrounding charge yields the surface tension, because it exerts only the Coulomb force with the central ion. We denote the surrounding charge in the latter state by $-\omega_i$ for the central ion i . Hence, the surrounding charge in the former state is $-(z_i - \omega_i)$. If the interparticle forces are restricted to the Coulomb force and the short-range repulsive force, the actual surface tension γ of a molten salt can be obtained by summing up the Coulomb forces between an arbitrary central ion having the charge of z_i and the separated surrounding charge of $-\omega_i$, and it is given by

$$\begin{aligned}\gamma &= -(e^2/32) \sum_i z_i (-\omega_i) n_i \\ &= (e^2/32) \omega \sum_i |z_i| n_i\end{aligned}\quad (6)$$

where ω is the average value of $|\omega_i|$ for the salt system under consideration.

Tables III and IV show the values of ω for typical halides calculated by eq 6 from the published values of surface tension.^{10,18} It is very interesting that all the ω values do not depend on the ionic valence of the salt melt and are around 0.5 at relevant temperature. In the case of bivalent central ions, the increasing charge of the central ion seems not to increase the separated surrounding charge but to increase the contacting one.

At this stage, it can be concluded that ω does not change sensitively with the valence of the central ion although it moderately depends on the ionic size parameter and tem-

perature. For simplicity, ω is regarded roughly later as a constant value of 0.5 for all the salt melts.

Now we shall compare the present experimental results with the calculated values by eq 6. Assuming there exist only the ions Li^+ , Be^{2+} , and F^- in the $\text{LiF}-\text{BeF}_2$ binary melt and denoting the mole fraction of BeF_2 by x , the number densities of each ions, n_{Li^+} , $n_{\text{Be}^{2+}}$, and n_{F^-} are respectively

$$\begin{aligned}n_{\text{Li}^+} &= (1-x)N_A/V_m \\ n_{\text{Be}^{2+}} &= xN_A/V_m \\ n_{\text{F}^-} &= (1+x)N_A/V_m\end{aligned}\quad (7)$$

where N_A and V_m are the Avogadro number and the molar volume of the melt, respectively. With ω of 0.5 and the number densities of ions given by eq 7, eq 6 gives an isotherm of $\text{LiF}-\text{BeF}_2$ binary melts at 800 °C as shown by the broken curve in Figure 3. There is an apparent discrepancy between the measured and calculated values.

This discrepancy will be explained as follows by considering the possibility of the formation of a complex ion. The above calculation was based on the assumption that the system is composed of Li^+ , Be^{2+} , and F^- . However, the strong polarizing power of Be^{2+} might lead to the formation of a complex ion. In fact, it has been known from the X-ray diffraction pattern that there may be a complex ion such as BeF_4^{2-} in the system containing beryllium.² This evidence may allow us to expect the presence of BeF_4^{2-} in the melt. Assuming that when $0 \leq x \leq 1/3$ all Be^{2+} ions form BeF_4^{2-} and when $1/3 \leq x \leq 1$ all F^- ions combine with Be^{2+} to form BeF_4^{2-} , the number densities of the species in the melt are expressed by eq 8. The recalculated

for $0 \leq x \leq 1/3$

$$\begin{aligned}n_{\text{Li}^+} &= (1-x)N_A/V_m \\ n_{\text{BeF}_4^{2-}} &= xN_A/V_m \\ n_{\text{F}^-} &= (1-3x)N_A/V_m\end{aligned}$$

for $1/3 \leq x \leq 1$

$$\begin{aligned}n_{\text{Li}^+} &= (1-x)N_A/V_m \\ n_{\text{Be}^{2+}} &= -1/4(1-3x)N_A/V_m \\ n_{\text{BeF}_4^{2-}} &= 1/4(1+x)N_A/V_m\end{aligned}\quad (8)$$

surface tension isotherm is shown by the solid curve in Figure 3. A satisfactory agreement is found between the recalculated and measured values. Thus, it is concluded that the complex ions BeF_4^{2-} are formed in the surface layer of the $\text{LiF}-\text{BeF}_2$ binary melt and have a definite influence on the surface tension.

Conclusion

The surface tension of $\text{LiF}-\text{BeF}_2$ binary melt has been measured by the maximum bubble pressure method and its isotherm shows a large negative deviation from additive behavior.

From the systematic consideration of the surface tension data of molten halides an empirical equation (eq 6) has been introduced and it predicts quantitatively to some extent the surface tension of molten halides containing no complex ions. For $\text{LiF}-\text{BeF}_2$ binary melt, this equation fairly gives the value of surface tension when the presence of complex ion BeF_4^{2-} is taken into account.

Acknowledgment. We thank Messrs. H. Yano and T. Hara for their cooperation in the experiment. Thanks are also due to Professor Y. Itoh for valuable discussions.